


Groundwater evaluation of northern Jazmourian (south Iran) for drinking, agriculture, and associated health risks of nitrate and fluoride contamination

Behnam Abbasnejad, Ahmad Abbasnejad & Reza Derakhshani

To cite this article: Behnam Abbasnejad, Ahmad Abbasnejad & Reza Derakhshani (2023) Groundwater evaluation of northern Jazmourian (south Iran) for drinking, agriculture, and associated health risks of nitrate and fluoride contamination, Human and Ecological Risk Assessment: An International Journal, 29:1, 36-57, DOI: [10.1080/10807039.2022.2140028](https://doi.org/10.1080/10807039.2022.2140028)


To link to this article: <https://doi.org/10.1080/10807039.2022.2140028>

 View supplementary material 

 Published online: 07 Nov 2022.

 Submit your article to this journal 

 Article views: 30

 View related articles 

 View Crossmark data 



Groundwater evaluation of northern Jazmourian (south Iran) for drinking, agriculture, and associated health risks of nitrate and fluoride contamination

Behnam Abbasnejad^a , Ahmad Abbasnejad^a , and Reza Derakhshani^{a,b}

^aDepartment of Geology, Shahid Bahonar University of Kerman, Kerman, Iran; ^bDepartment of Earth Sciences, Utrecht university, Utrecht, Netherlands

ABSTRACT

To investigate groundwater quality in the north of Jazmourian (Roudbar plain), 30 samples were collected and analyzed for evaluating drinking and irrigation status and associated health risks. In addition to major anions and cations, the fluoride and nitrate content of samples were analyzed using standard procedures. Nitrate levels range between 6.6 and 131 mg/L and exceed the WHO permissible limit in more than 23% and 80% of samples for adults and children, respectively. Fluoride amounts ranged from 0.4 to 4.8 mg/L in samples. The F^- level exceeded the WHO standard limit in 10% of samples. The EC level increases in fine-grained deltaic deposits toward the south. The concentrations of major ions (HCO_3^- , Cl, SO_4 , Mg, Na, K) increase southwards, following the flow direction. There are, however, lateral (east-west) differences in water quality due to the influence of such factors as the rate of recharge and the type of bedrock. Wherever the redbeds comprise the bedrock and the recharge rate is weaker, the dissolved salts are higher in amount. The water quality index (IWQ) indicated that 13, 13, and 4 samples are in “good,” “poor,” and “very poor” quality classes, respectively. By using the irrigation water quality index (IWQI), eight samples were at “low restriction,” nine samples at “moderate restriction,” twelve samples at “high restriction,” and one sample at “severe restriction” classes. The acquired findings revealed that the mean oral hazard quotient of nitrate was 1.14, 1.0, and 0.84, and for fluoride, it was 0.82, 0.72, and 0.61 for children, females, and males, respectively. The total hazard index for cumulative NO_3^- and F^- toxicity exceeded the acceptable level in 76.67%, 66.67%, and 56.67% of samples for children, females, and males, respectively.

ARTICLE HISTORY

Received 26 August 2022
Revised manuscript
Accepted 20 October 2022

KEYWORDS

Roudbar; groundwater pollution; noncarcinogenic health risk; F^- contamination

Introduction

Supplying safe drinking water is a basic requirement for the development of human societies. Groundwater is the main source of consuming water in dry and semidry countries (Qasemi et al. 2019). About two-thirds of the global population depends on groundwater resources for agriculture, drinking, and industrial water demands

CONTACT Ahmad Abbasnejad aabbas@uk.ac.ir Shahid Bahonar University of Kerman, Kerman, Iran.

Supplemental data for this article can be accessed online at <https://doi.org/10.1080/10807039.2022.2140028>

© 2022 Taylor & Francis Group, LLC

(Adimalla et al. 2019). In Iran, groundwater is the main source of water supplements. In recent years, however, such factors as drought and overdraft have led to groundwater quantity reduction and quality deterioration. Groundwater quality in both rural and urban areas is deteriorating due to such factors as pollution by sewage, septic tanks, and agriculture (Rezaei et al. 2019).

Nitrate and fluoride are considered the most widespread contaminants in groundwater (Adimalla and Venkatayogi 2018). Nitrate pollution is the most abundant and probably the most common form of groundwater pollution in hot and dry areas (Bahrami et al. 2020). It originates from several natural and anthropogenic sources. Agricultural and industrial wastewaters, landfill leachates, urban run-off, as well as animal wastes are considered the main sources of nitrate pollution in groundwaters (Adimalla and Li 2019). High intakes of nitrate may lead to abortion as well as a decrease in oxygen transfer to the fetus via maternal blood (Chetty and Prasad 2016). WHO (2017) has set the standard level of nitrate in water at 50 mg/L for adults and 15 mg/L for infants. Exposure to high levels of nitrate may cause some health problems such as methemoglobinemia (blue baby syndrome) as well as gastric, esophagus, and ovarian cancers (Bao et al. 2017). High nitrate exposure during pregnancy might result in miscarriage. Other diseases related to elevated nitrate levels include hypertrophy of the thyroid, and coronary cardiac disease (Gangolli et al. 1994).

The presence of fluoride in groundwater is a normal occurrence and its level is affected by local and regional conditions. In addition to natural factors, anthropogenic sources can also increase the concentration of this element in groundwater. The main human sources of fluoride pollution include agricultural fertilizers, effluents of metallurgic industries, as well as coal combustion (Dehbandi et al. 2017).

Weathering of such rocks as basalt, granite, and shale usually increase the fluoride content of groundwaters. Minerals including fluorapatite, hornblende, apatite, muscovite, fluorspar, cryolite, and topaz contain fluoride in their structure (Mukherjee and Singh 2018). The concentration of fluoride in groundwater depends on such factors as the quality and dissolution of fluoride-bearing minerals, temperature, pH, salinity, vegetation, calcium, and bicarbonate levels in water; as well as anion exchange conditions (Appelo and Postma 2004).

Industrialization and population growth have raised the need for water. As a result, the assessment of water quality has gotten more attention. About 80% of all diseases across the world have resulted from the use of poor-quality water (Qasemi et al. 2019). Many nations have faced F^- and NO_3^- contaminated waters, some of them include India (Adimalla and Li 2019; Kumar 2021), China (Chen et al. 2017; Su et al. 2021), Pakistan (Arshad and Imran 2017; Hameed et al. 2021), and Sri Lanka (Rajasooriyar et al. 2013). Chen et al. (2016) studied nitrate pollution and associated health risk in Ningxia, China. They have reported nitrate concentration up to 62.2 mg/L and the NO_3^- sources were fertilizers, extensive irrigation, shallow aquifer, high permeability of the soil, poor sanitation, and inadequate infrastructure. In the groundwater study of the Ethiopia rift conducted by Haji et al. (2021), fluoride and nitrate levels reached 5.60 and 69.5 mg/L, and they concluded acidic volcanic rocks and agricultural activities are controlling factors for F^- and NO_3^- pollution, respectively. Chen et al. (2021) conduct a survey on fluoride behavior in the Yellow river basin and found evaporate dissolution and

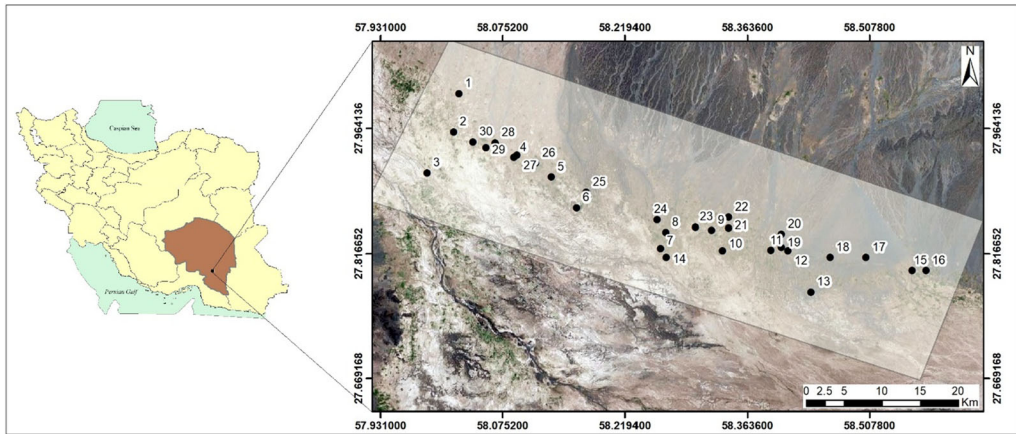


Figure 1. Map of study area showing the sampling locations.

evaporation were the dominant factors in F^- elevation, whereas carbonate weathering had a major role in groundwater regulation.

In Iran, some studies have been undertaken on NO_3^- and F^- pollution of groundwaters (Azhdarpoor et al. 2019; Bazeli et al. 2020). Additionally, several studies have been conducted on the co-occurrence of F^- and NO_3^- . As an example, Rezaei et al. (2017) have studied the hydrogeochemistry of groundwaters in the Lar region and have reported that F^- and NO_3^- concentration ranges are 0.59–3.92 and 1.47–70.66 mg/L, respectively. According to their study, groundwater quality in this area is affected by such processes as dissolution-precipitation of carbonates and evaporates; evaporation of water; as well as reverse ion exchange. In a study by Qasemi et al. (2022), the concentration of F^- and NO_3^- in Sabzevar was reported in the range of 0.197–1.32 and 8.8–47.2 mg/L, respectively. Rezaei et al. (2019) have reported 0.22–0.27 and 0.28–80 mg/L of fluoride and nitrate in the Sanandaj area. Toolabi et al. (2021) have reported the concentration of nitrate and fluoride in groundwaters of the Bam plain in the range of 8.5–10.85 and 0–91–1.12 mg/L, respectively, meaning lower concentrations than WHO standards.

In the northern part of Jazmourian, studies related to groundwater quality have not been carried out. Hence, this study aims to: (1) determine the concentration of F^- and NO_3^- and evaluate the spatial distribution of these ions in the groundwater of northern Jazmourian depression (known as the Roudbar plain); (2) evaluate the water quality of samples using WQI and associated potential health risks; and (3) assess irrigation water quality. These studies will provide valuable information for better planning of water resources and public health in such areas.

Study area

Location and climate

The study area is located in the southeast of Iran and covers an area about 70 km in length and 30 km in width (Figure 1). Its average altitude is about 500 m above sea level and slopes toward the south. In this area, precipitation varies from 200 mm/yr in the

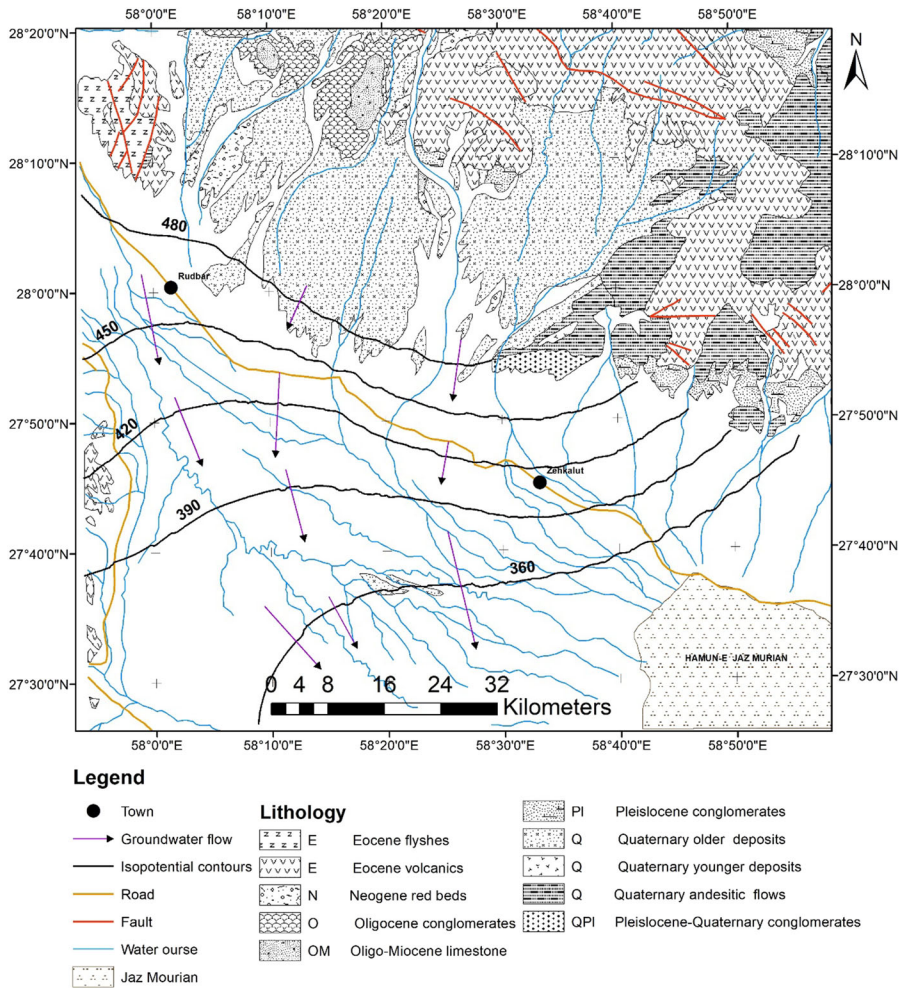


Figure 2. Geological map of the studied area.

lowlands (south) to about 400 mm/yr in the highlands (north). The annual average temperature of the plain is about 25 °C, indicating that the studied area is arid, with hot summers and mild winters. In this area, there are a couple of towns (Roudbar and Zehkalut) and about a dozen villages. The total living population is around 50,000 persons. Agriculture is the primary land use and activity. High rates of agricultural water evaporation result in salt-rich return flows that raise the TDS and nitrate level of groundwater (Nazerizadeh 2017).

Geology

The main lithological units of the area, as shown in Figure 2, are: (1) Eocene flyshes with small outcrops at the foothills, (2) andesitic, rhyolitic, dacitic, and basaltic flows as well as pyroclastics of Eocene age which are the main rocks comprising the mountains, (3) small outcrops of Oligo-Miocene conglomerates at the foothills, (4) Oligo-Miocene limestones which are encountered as scattered hills to the north of the studied area, (5)

Neogene red beds, (6) Pliocene conglomerates, and (7) Pliocene-Quaternary conglomerates which outcrop at some locations in piedmont areas, (8) Quaternary andesitic flows at the northeast and (9, 10) old and young Quaternary gravels which take their place to deltaic sediments (sands, silts, and clays) toward the south. All the aforementioned 1 to 5 rock units serve as bedrock of the alluvial aquifer in various parts. However, wherever the Neogene redbeds which contain evaporitic minerals (gypsum and halite) are in contact with the aquifer, groundwater is richer in dissolved salts.

Hydrogeology

The hydrogeology of the studied area is investigated by Nazerizadeh (2017). In this area which is located at the north of the Jazmourian depression, quaternary alluvials play as the aquifer. These alluvials which are fan deposits in the north and deltaic deposits in the south have resulted from the erosion of the Jabal-barez mountains in the north. These mountains are mainly comprised of folded and faulted Eocene volcanic rocks.

The aquifer is replenished from the north, mainly via valley-bottom alluvials, but spreading floods over the alluvial fans play as a subsidiary agent of aquifer replenishment. Groundwater flows from the north toward the south, but it deflects toward the southeast in the southern parts of the area.

At the north of study area, the alluvials comprising the aquifer are mainly coarse gravel. They gradually give their place to deltaic sand, silt, and clay layers at the south. In these deltaic deposits, the sandy layers play as aquifer and, considering the interbedded clay layers are thin and pinch out toward the recharge zone (north), differences of groundwater quality among these sandy layers are supposed to be very slight.

The depth of bedrock is very variable in the alluvial fan environment in the north. However, toward the deltaic environment in the south, the depth of bedrock is unknown and it is estimated to be in excess of 300 m. Groundwater depth varies from about 60 m in the north of the study area to about 40 m in the south. Presently, the water level in this area is falling at an average rate of about 1 m per year, mainly because of overdraft and drought conditions.

The samples taken from the wells drilled in alluvial fan deposits belong to the same layer, but toward the delta environment, there are thin layers and lenses of clay among sandy layers.

The aquifer is mainly recharged from the north and groundwater flows toward the south and southeast. Before extraction by drilled wells, groundwater was discharged as seepage into the Jazmourian lagoon (Hamun-E Jazmourian) located in the southeast (Figure 2). However, presently, extraction by around 200 drilled wells is so large that discharge into the lagoon is interrupted and the lagoon has almost dried up.

Materials and methods

Sampling was performed on one day in March 2019. Samples were collected from producing wells which are mainly concentrated in a zone around the main road of the studied area, where both soil fertility and well discharge are in the best conditions. For sampling, a couple of 1-liter polyethylene bottles were used at each station. Before

sampling, the pump was turned on for at least 15 min, and the bottles were rinsed with sampling water. Water temperature, EC, and pH were measured at the field with a calibrated set (Evtech – PCD 650) and geographical coordination was determined using a GPS set (Garmin, eTrex-vista). Water samples for anion analysis were filtered using 0.45 micron filter papers, and the bottles considered for cation and heavy metal analyses were acidified to $\text{pH} < 2$ using 65% nitric acid.

Laboratory analysis and quality assurance

Potential toxic metals and cations were measured using the inductively coupled plasma mass spectrometry (ICP-MS) method (HP-Agilent 4500 device) in Zarazma laboratory, Tehran, Iran. SO_4 concentrations were determined using spectrophotometry (DR 2500, HACH, USA). Carbonate and chloride concentrations were determined by titration and AgNO_3 titration, respectively. Nitrate concentration was determined by spectrophotometry (DR 2500-HACH). In this method, 1 cc of the sample was mixed with acid containing 12.5 gram phenol, 75 cc duty sulfuric acid, and 37.5 cc fuming sulfuric acid in a beaker. Afterwards, 2 cc of this sample was mixed with 10 cc of ammoniac, and the changed color was compared with the standard. Fluoride concentrations were determined using the spectrophotometry SPANDS method. In this method, F^- is combined with a Zr-bearing compound, and ZrF_6^{2-} complexes are formed. This mixing reduces the color of the samples and is positively related to the concentration of F^- . Then, absorbance was determined spectrophotometrically at the wavelength of 570 nm. The standard curve was finally drawn for F^- in mg/L.

To check the accuracy and precision of analyses, a duplicate sample was taken after taking every 10 samples, that is, a total of three samples were analyzed for QA/QC. For precision of analyses, CRM samples were used in the Zarazma laboratory. Finally, relative standard deviations (RSD) were calculated. All parameters had RSD in the range of 90–98. Additionally, charge balance errors were calculated for all parameters, which were in the acceptable range (± 5).

Water quality index

Water quality index (WQI) is a practical tool to assess overall surface and groundwater quality which was introduced by Horton (1965) and modified by Brown et al. (1970). This index is widely used throughout the world (Jabbo et al. 2022; Khalid 2019; Zhang et al. 2020). To calculate WQI, some of the key parameters of groundwater on the basis of their relative importance were used. The main physicochemical parameters which play important role in the water quality calculated in this study included: Ca, Mg, Na, K, HCO_3 , SO_4 , Cl, NO_3 , EC, pH, F, TDS, and As. By this means, a large set of water quality data reduces into indicative and comprehensive numbers. The assigned weight depends on the importance of mentioned parameter in overall water quality and human health. In the current research, weight and standard values were used based on the world health organization report (WHO 2017) (Table 1). Afterward, WQI was computed in the following steps:

Table 1. The weight (w_i) and relative weight (W_i) of parameters used for WQI.

Parameter	Unit	WHO standard	Weight (w_i)	Relative weight (W_i)
Ca	mg/L	75	2	0.043
Mg	mg/L	50	2	0.043
Na	mg/L	200	3	0.065
K	mg/L	12	2	0.043
HCO ₃	mg/L	250	3	0.065
SO ₄	mg/L	250	4	0.087
Cl	mg/L	200	3	0.065
NO ₃	mg/L	50	5	0.109
As	mg/L	10	5	0.109
F	mg/L	1.5	5	0.109
EC	μmohs/cm	1000	3	0.065
TDS	mg/L	1000	5	0.109
pH		7	4	0.087

The relative weight of each parameter is calculated according to Eq. (1):

$$W_i = \frac{w_i}{\sum_{i=1}^n w_i} \quad (1)$$

where W_i , w_i , and n are the relative weight, the weight of each parameter, and the number of parameters, respectively.

The quality rating scale (q_i) for each parameter was calculated by dividing its concentration by corresponding values of WHO guidelines and the result was multiplied by 100, as follows:

$$q_i = \left(\frac{C_i}{S_i} \right) \times 100 \quad (2)$$

where C_i and S_i represent the concentrations of each distinctive parameter in each water sample and the WHO drinking water quality standard for each chemical parameter, respectively. SI_i and WQI were then determined for each parameter using Eqs. (3) and (4):

$$SI_i = W_i \times q_i \quad (3)$$

$$WQI = \sum_{i=1}^n SI_i \quad (4)$$

WQI has five classes:

Excellent <50, good 50–100, poor 100–200, very poor 200–300, and >300 unsuitable drinking water.

Irrigation water quality

Given that groundwater is the only source of water for irrigation in this region, its quality for irrigation is assessed. For this purpose, the irrigation water quality index (IWQI) of samples was calculated. This model was first introduced by Meireles et al. (2010) and numerous researchers have utilized it for irrigation water quality studies (Abbasnia et al. 2019; Aravinthasamy et al. 2020; Khalaf and Hassan 2013). The privilege of this

Table 2. Limit values of quality measurement (q_i).

q_i	CE ($\mu S/cm$)	SAR (meq/L) ^{1/2}	Na ⁺ (meq/L)	Cl ⁻ (meq/L)	HCO ₃ ⁻ (meq/L)
85–100	200 ≤ EC < 750	2 ≤ SAR < 3	2 ≤ Na < 3	1 ≤ Cl < 4	1 ≤ HCO ₃ < 1.5
60–85	750 ≤ EC < 1500	3 ≤ SAR < 6	3 ≤ Na < 6	4 ≤ Cl < 7	1.5 ≤ HCO ₃ < 4.5
35–60	1500 ≤ EC < 3000	6 ≤ SAR < 12	6 ≤ Na < 9	7 ≤ Cl < 10	4.5 ≤ HCO ₃ < 8.5
0–35	0–35 EC < 200 or EC ≥ 3000	SAR < 2 or SAR ≥ 12	Na < 2 or Na ≥ 9	Cl < 1 or Cl ≥ 10	HCO ₃ < 1 or HCO ₃ ≥ 8.5

Source: Meireles et al. (2010)

method is that it incorporates all of the major influencing irrigation factors into its calculations. Therefore, it illustrates the general quality of irrigation water.

To calculate this index, the relative weight of each factor is determined, and then, the permissible values and concentration limit of the parameter are used to determine the coefficient for each factor. The IWQI is calculated by adding these coefficients together. For this purpose, an aggregation weight (w_i) and quality measurement values (q_i) definition have been established. q_i and w_i values were determined for each parameter according to irrigation water criteria established by the university of California committee of consultants and Ayers and Westcot (1985) and listed in Table 2. According to the parameters in Table 2 and the results of the analyzed sample’s concentrations, values of q_i were calculated using Eq. (5).

$$q_i = q_{i\max} - [(x_{ij} - x_{\inf}) \times q_{iamp}] / q_{amp} \tag{5}$$

where $q_{i\max}$ represents the maximum value of q_i for the class; x_{ij} denotes the observed value of the parameter; x_{\inf} indicates the corresponding value to the lower limit of the class to which the parameter belongs, q_{iamp} is class amplitude, and q_{amp} exhibits class amplitude to which the parameter belongs. Consequently, w_i values were normalized to be equal to one in accordance with Eq. (6):

$$w_i = \frac{\sum_{j=1}^k F_j A_{ij}}{\sum_{j=1}^k \sum_{i=1}^n F_j A_{ij}} \tag{6}$$

where w_i represents the weight of the parameter for the WQI; F denotes component 1 autovalue; A_{ij} signifies the explainability of parameter i by factor j ; i indicates the number of physico-chemical parameters selected in the model, ranging from 1 to n ; and j represents the number of factors selected in the model, varying from 1 to k . The relative weights assigned to each parameter are shown in Table 3.

Ultimately, IWQI can be calculated using q_i and w_i for each groundwater sample. The IWQI ranges from 0 to 100 and is a dimensionless parameter. The irrigation water quality index was determined by the following Equation:

$$IWQI = \sum_{i=1}^n q_i \times w_i \tag{7}$$

where q_i denotes the quality of the i th parameter and is related to its concentration, which ranges between 0 to 100, and w_i is the normalized weight assigned to the i th parameter, based on its significance in explaining global water quality variability. The WQI has considered the risk of salinity issues, soil water infiltration reduction, as well as

Table 3. Weights for the IWQI parameters.

Parameters	w_i
Electrical conductivity (EC)	0.211
Sodium (Na ⁺)	0.204
Chloride (Cl ⁻)	0.194
Bicarbonate (HCO ₃ ⁻)	0.202
SAR	0.189
Total	1.00

Source: Meireles et al. (2010)

Table 4. Exposure factors for health risk assessment of groundwater via ingestion pathway.

Exposure variable	Unit	Children	Female	Male
IR	L/day	0.78	2.5	2.5
EF	day/year	365	365	365
ED	Year	12	67	64
W	kg	15	55	65
AT	day	4380	24,445	23,630

toxicity to plants. Levels of restriction on water use were identified in various classes (Supporting Information Table S1) (Meireles et al. 2010).

Health risk assessment

The risk of potentially toxic compounds in water is a crucial aspect that has received extensive research (Abbasnejad et al. 2013; Adimalla and Qian 2019; Enalou et al. 2018). The majority of these compounds may threaten human health via three pathways which include ingestion, inhalation, and dermal contact. For drinking water purposes, ingestion is the primary route.

Nitrate and fluoride are considered toxic when used in excess of safe levels; the exposure risk of these two chemicals can be calculated as follows.

$$\text{Ingestion}_{\text{oral}} = \frac{\text{CW} \times \text{IR} \times \text{EF} \times \text{ED}}{\text{BW} \times \text{AT}} \quad (4)$$

where the CW is concentration, IR is ingestion rate, EF is exposure frequency, ED is exposure duration, BW is bodyweight, and AT is average exposure time for noncarcinogenic chemicals (Table 4).

To determine noncarcinogenic contamination caused by contaminated water, hazard quotient (HQ) and reference dosage (RfD) are used. The calculated oral risks are used to determine the noncarcinogenic effect of nitrate and fluoride separately, as follows:

$$\text{HQ} = \frac{\text{oral intake}}{\text{RfD}_{\text{oral}}} \quad (5)$$

The RfD or oral reference dose for nitrate and fluoride are 1.6 and 0.06 mg/kg, respectively (Li et al. 2016). The permissible risk for nitrate and fluoride is $\text{HQ} < 1$, and if $\text{HQ} \geq 1$. It represents the noncarcinogenic impact of these chemicals. The total hazard index (THI) imposed by both these chemicals is:

$$\text{THI} = \text{HQ}_{\text{nit}} + \text{HQ}_{\text{Flu}} \quad (6)$$

Table 5. Statistical summary of physicochemical parameters in groundwater samples.

Station	Ca mg/L	K mg/L	Mg mg/L	Na mg/L	SO ₄ mg/L	NO ₃ mg/L	HCO ₃ mg/L	Cl mg/L	F mg/L	T (°C)	EC (µmoh/cm)	pH
1	1.6	2.9	7.3	414.4	408.9	8.9	170.8	383.4	1.2	31.0	1200.0	7.7
2	378.5	6.1	58.4	821.4	1424.9	70.7	189.1	976.2	0.7	28.0	4850.0	7.3
3	68.3	5.5	50.8	943.0	1164.3	32.8	305.0	713.5	2.0	28.0	4300.0	7.7
4	45.0	3.3	5.5	261.4	425.9	8.0	91.5	142.0	0.5	32.0	1350.0	6.5
5	65.1	2.7	13.7	409.9	491.2	64.9	170.8	337.2	0.7	31.0	2150.0	6.8
6	164.4	4.4	43.3	866.9	1318.5	36.6	336.0	564.4	4.8	29.0	4170.0	7.1
7	184.9	4.9	35.5	654.9	1080.1	15.5	109.8	603.5	0.4	30.0	3720.0	7.1
8	394.5	5.7	66.0	670.6	1643.3	131.0	183.0	639.0	0.4	30.0	4500.0	7.1
9	83.4	6.2	27.7	282.0	401.9	44.2	134.2	301.7	4.8	31.0	1767.0	6.9
10	263.6	10.2	92.1	520.2	971.2	49.8	262.3	674.5	0.4	30.0	3760.0	6.8
11	73.0	3.6	25.9	160.5	263.2	53.9	183.0	159.7	0.4	30.0	1210.0	6.8
12	47.3	3.1	12.7	119.8	133.1	17.4	213.5	88.7	0.4	33.0	815.0	6.7
13	86.3	3.2	32.8	250.3	387.5	22.4	201.3	241.4	0.4	31.0	1644.0	6.5
14	86.7	7.8	28.3	182.4	181.7	33.0	183.0	287.5	0.4	33.0	1452.0	6.6
15	76.0	4.5	23.0	140.5	251.6	19.7	176.9	138.4	0.4	28.0	1149.0	6.9
16	67.0	4.9	19.8	368.5	587.3	23.0	250.1	181.0	0.4	30.0	1890.0	7.1
17	47.8	5.5	15.4	138.3	153.3	21.9	170.8	138.4	0.4	30.0	977.0	6.9
18	39.9	6.3	13.8	155.1	174.3	19.7	183.0	124.2	0.4	32.0	994.0	6.7
19	60.6	3.4	18.5	139.9	173.5	43.9	213.5	131.3	0.6	31.0	1078.0	7.2
20	37.6	3.6	13.7	152.8	168.2	32.8	195.2	113.6	0.6	31.0	956.0	6.8
21	225.3	6.9	79.8	583.0	371.0	10.9	109.8	1207.0	0.5	32.0	4210.0	7.5
22	38.8	4.1	15.0	167.3	185.0	13.0	201.3	124.3	1.0	33.0	1007.0	7.0
23	185.1	5.9	50.0	509.2	735.4	38.8	183.0	628.3	0.8	30.0	3330.0	7.7
24	47.6	2.7	8.1	276.4	380.9	29.8	176.9	159.7	0.8	30.0	1340.0	6.9
25	58.0	3.6	12.8	414.5	540.0	42.9	128.1	319.5	0.8	32.0	2190.0	7.2
26	40.4	2.7	7.2	335.3	372.6	56.1	183.0	237.8	1.0	30.0	1704.0	6.9
27	21.0	2.4	3.5	213.0	234.8	6.6	176.9	106.5	0.8	30.0	1084.0	7.2
28	64.5	2.2	10.2	261.6	324.8	65.2	170.8	216.5	0.7	30.0	1550.0	7.1
29	34.4	2.2	5.4	285.3	238.1	27.4	164.7	252.0	0.8	30.0	1445.0	6.9
30	85.5	2.6	13.0	338.7	335.2	12.8	140.3	391.5	1.0	30.0	2008.0	7.1
Min	1.6	2.2	3.5	119.8	133.1	6.6	91.5	88.7	0.4	28.0	815.0	6.5
Max	394.5	10.2	92.1	943.0	1643.3	131.0	336.0	1207.0	4.8	33.0	4850.0	7.7
Mean	102.4	4.4	27.0	367.9	517.4	35.1	185.3	352.8	1.0	30.5	2126.7	7.0
Median	66.05	3.85	16.95	283.65	376.75	31.3	183	246.7	0.65	30	1597	6.95

Statistical and spatial analysis

In this study, statistical analysis was performed using Microsoft Excel 2019 and SPSS 24.0. Also, AqQA 1.5.0, and Rockworks 16 softwares were used to calculate water types. The irrigation quality of water samples was calculated by IWQI software 1.8.1. The ArcGIS (Ver. 10.4) was employed to generate the spatial distribution maps.

Results and discussion

General hydrogeochemistry

Statistical summaries of physicochemical characteristics of samples are presented in Table 5. The pH ranges of samples are 6.5–7.7, meaning neutral waters (Figure 3a). The EC ranges between 815 and 4850 µs/cm, with a mean of 2127 µs/cm. As Figure 3b reveals, EC decreases from west to east, the reason is assumed to be dilution as a result of recharge by large alluvial fans in the east. The lowest and highest levels of TH are 67 and 1257 mg/L, respectively. The highest levels are observed at the central parts, where evaporite-bearing bedrocks are present (Figure 3c). Generally, the shares of the soft, moderate, hard, and very hard waters are 3.33, 6.67, 23.33, and 66.67, respectively.

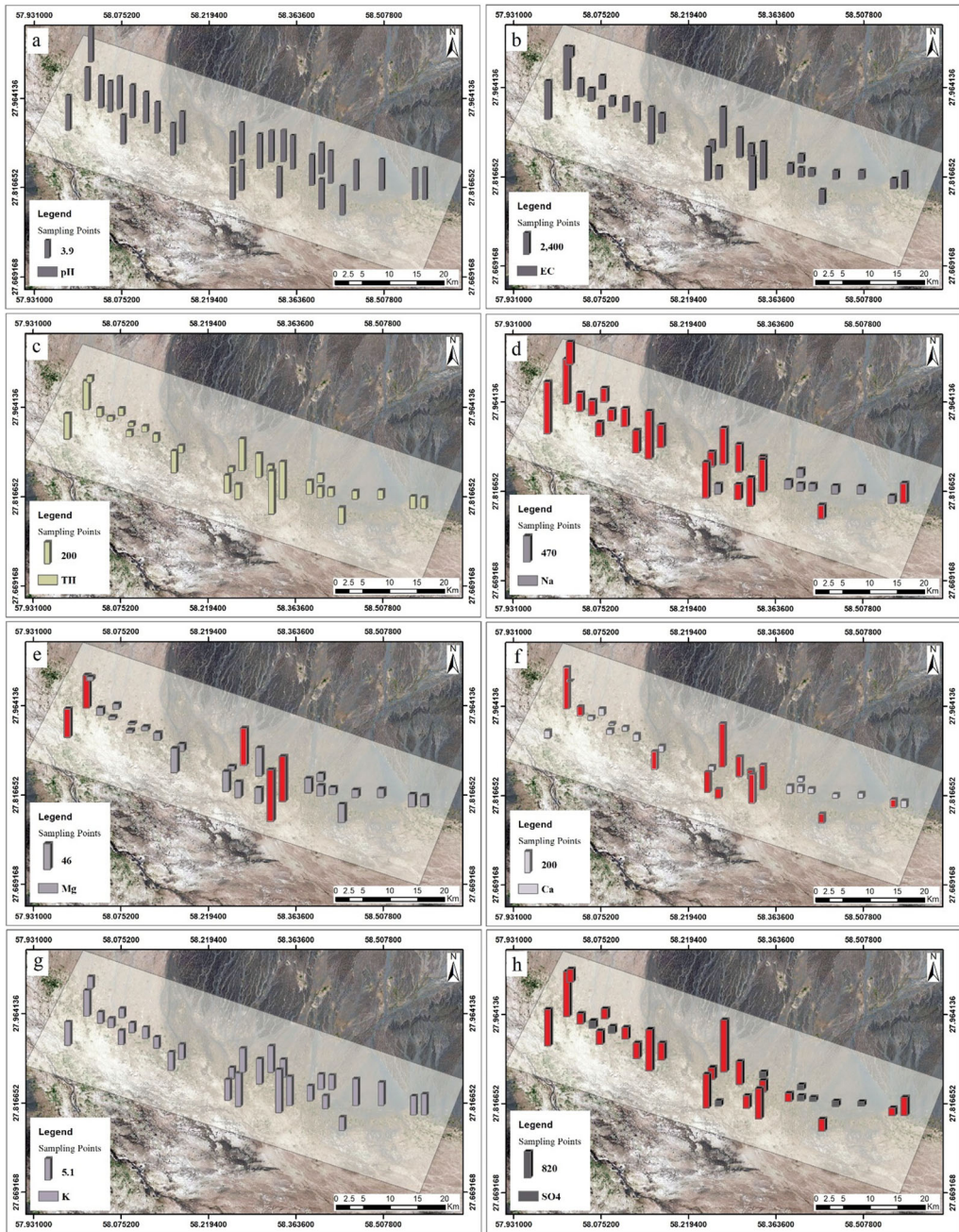


Figure 3. Spatial distribution of (a) pH, (b) EC, (c) TH, (d) Na, (e) Mg, (f) Ca, (g) K, (h) SO₄, (i) Cl, (j) HCO₃, (k) NO₃, (l) F.

The site-wise variation diagram of samples is shown in [Figure 4](#). The abundance of ions is $SO_4 > Na > Cl > HCO_3 > Ca > NO_3^- > K > F^-$. As [Figure 4](#) depicts, the sum of concentrations is higher in the first 10 sampling points which are located in the west. Sodium level decreases toward the east ([Figure 3d](#)) and its minimum and maximum level are 120 and 943 mg/L, respectively, with an average value of 368 mg/L which, in

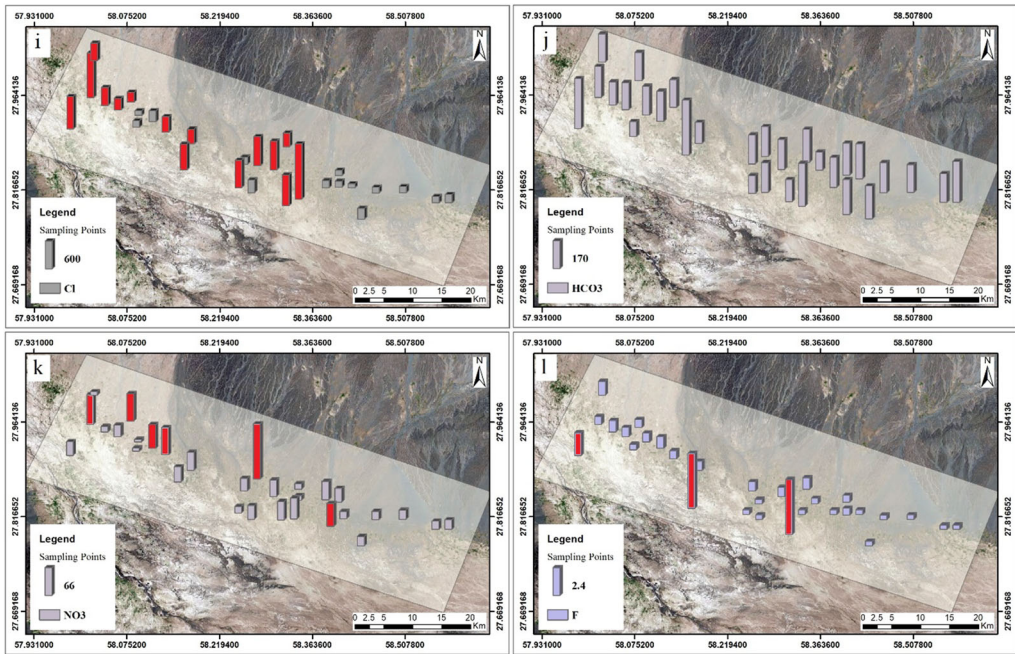


Figure 3. Continued.

comparison with the WHO (2017) standard (200 mg/L), is considerably higher due to such factors as evaporite dissolution, evaporation, and irrigation. As a result of evaporite bedrocks, the Mg^{2+} levels reach up to 92.1 mg/L in this area. Its mean value is 26.9 mg/L as a result of the influence of Mg-poor rocks in the west (Figure 3e). The distribution of Ca^{2+} is similar to Mg^{2+} , but the average is 104.5 mg/L, while the allowable level of WHO (2017) is 200 mg/L (Figure 3f). K^+ ranges are 2.17–10.16 mg/L, respectively, while its acceptable value is 12 mg/L (WHO 2017). As shown in Figure 3g, K^+ has higher levels in central parts since its variation is mainly due to the influence of agricultural fertilizers.

Among anions, sulfate with an average of 517 mg/L has the highest concentration. Given its WHO permissible value is 250 mg/L; 22 samples (73.33%) exceed this level. As illustrated in Figure 3h, higher concentrations of this anion are observed in the south-west, probably as a result of evaporative dissolution. Chloride concentration ranges between 88.7 and 1207 mg/L, which in 18 samples is higher than the 250 mg/L recommended level (WHO 2017). While, in six samples (2, 3, 8, 10, 21, 23) Cl level is higher than the desirable limit for agricultural uses which is 600 mg/L. As presented in Figure 3i, its concentration in the western and central parts of the plain are higher which shows the increased contribution of evaporite dissolution. HCO_3^- level varies between 91.5 and 366 mg/L which shows lower variation than other anions (Figure 3j), and all samples except a couple of them are below the permissible threshold of 300 mg/L (WHO 2017).

Nitrate levels range between 6.6 and 131 mg/L with an average value of 35.07 mg/L. This means rather large variations in its concentration. The reason is differences in agricultural density (nitrate pollution rate) and the rate of dilution of agricultural return flows by groundwater. In strong recharge zones, the return flows are mixed with a larger amount of groundwater and become more diluted. The highest concentrations

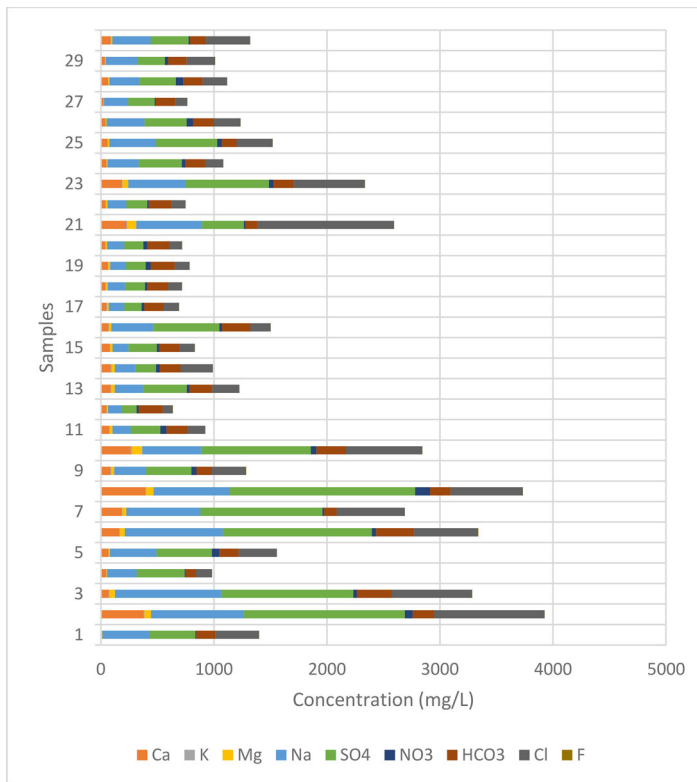


Figure 4. Site-wise variation of major anions and cations in groundwater samples of the study area.

are observed in samples 8 and 2 with 131 and 70.7 mg/L, respectively. These samples also contain high levels of Cl^- , Ca^{2+} , EC, Mg^{2+} , Na^+ , and SO_4^{2-} supposedly as a result of such factors as agricultural return flow and evaporite dissolution. The WHO allowable limit of nitrate level for adults is 50 mg/L and six samples (20%) exceed this level. However, the standard level for children is 15 mg/L and only six samples have lower NO_3^- content (80% of samples are polluted). As shown in Figure 3k, the highest concentration of nitrate was detected in central areas, where nitrate released by human activities (sewage and fertilizers) is higher and the dilution rate is lower than in other areas.

The fluoride concentration in water samples varies from 0.4 to 4.8 mg/L from the west to the east and the average is 0.95 mg/L (Figure 3l). Concentrations in three samples (3, 6, and 9) were above the permissible limit of 1.5 mg/L (WHO 2017). One sample (No. 9) lies at 1–3 mg/L class (dental fluorosis) and two samples (No. 3 and 6) lie at the 4–6 mg/L class (deformation in the knee and hip bones) (Murray 1986; Singh et al. 2020). In two samples (3 and 6) the CO_3^- and Na^+ levels are also high. This means that these ions support the release of F^- via controlling the dissolution of fluorite and other F-bearing minerals. High levels of Na in these samples may be the result of Aluminosilicate dissolution which influences the dissolution of F-bearing minerals through the production of OH^- and Na^+ ions. A volcanic belt at the north of the studied area may influence F^- levels in groundwaters. F^- concentration in water samples varies from 0.4 to 4.8 mg/L. The fluoride level in some samples related to the delta environment is higher. Based on such diagnostic plots as $\text{Na}/\text{Na} + \text{Cl}$ vs. TDS and the Cl vs. Na plot

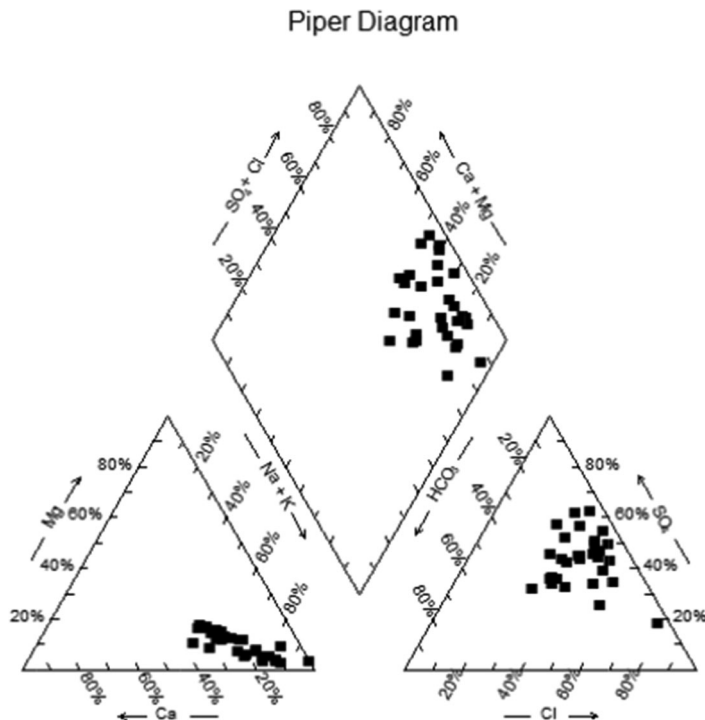


Figure 5. Piper trilinear diagram for groundwater samples from study area.

(Supporting Information [Figure S1](#)), ion exchange is happening in deltaic deposits. This process raises the Na^+ and falls the Ca^{2+} and Mg^{2+} content in groundwater. The consequent unsaturation with respect to fluorite has caused the dissolution of this mineral from the matrix. Additionally, a decrease in Ca^{2+} and Mg^{2+} content and an increase in Na^+ (stronger base) resulting from the ion exchange process increases OH^- . The exchange of OH^- with F^- adsorbed on mineral surfaces is another mechanism for high concentrations of fluoride.

To evaluate the geochemistry of groundwaters and dominant water types, the Piper diagram was used ([Figure 5](#)). The leftward triangle represents $\text{Na} + \text{K}$ type waters and the rightward triangle represents Cl^- and SO_4^{2-} types. The location of samples at the right of the main diamond indicates that groundwater quality in the study area is Na-Cl-SO_4 hydrochemical type. A stiff diagram of water samples ([Figure 6](#)) indicates that all samples lie in two groups which contain 70% of samples in Na-SO_4 type and the second one which includes about 30% of samples in Na-Cl type. Both groups indicate a strong influence on the dissolution of evaporite minerals containing gypsum and halite.

Water quality index

As noted, WQI illustrates some of the most important physicochemical parameters of groundwater into a single value, which is a simple indicator for comparing and characterizing the condition of samples. In evaluating WQI, the weight of each parameter, relative weight, and WHO guideline values are given in [Table 1](#).

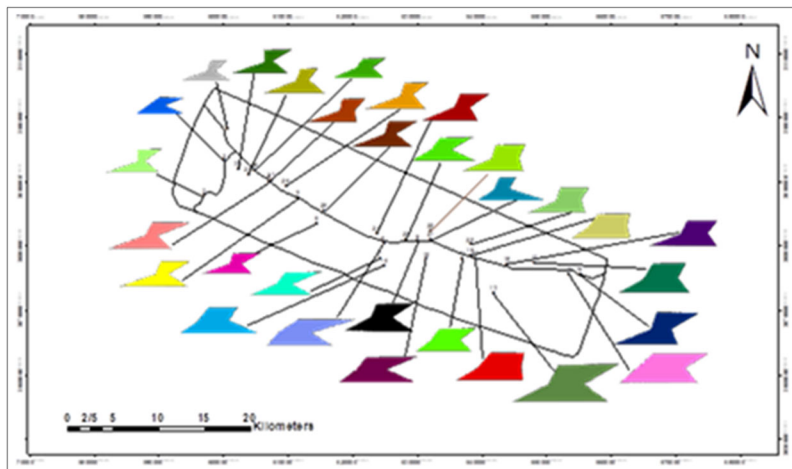


Figure 6. Spatial distribution map of Stiff diagram for groundwater samples.

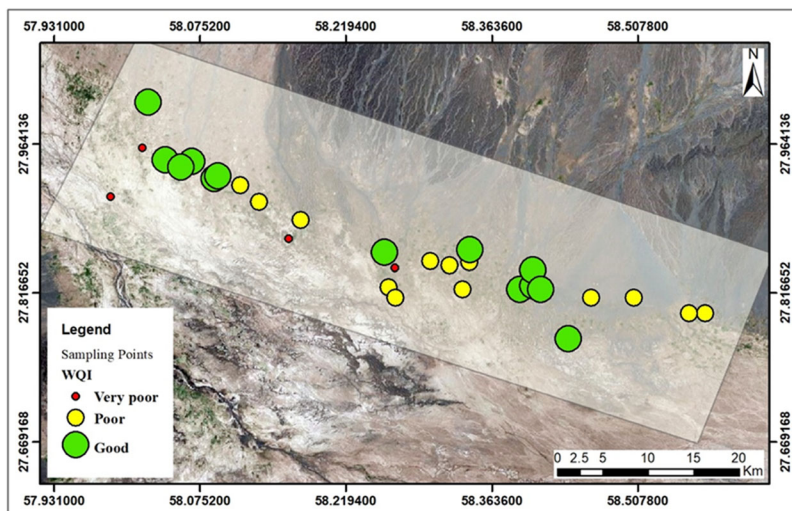


Figure 7. Spatial variation map of WQI.

The calculated values for WQI vary from 60.73 to 239.19. The results reveal that 13 samples were within the “good” water quality class and 13 samples were in the “poor” quality class (Figure 7). Additionally, four samples (No. 2, 3, 6, and 8) come under the “very poor” quality class. None of the groundwater samples meet the requirement of excellent water.

Irrigation water quality index

Using IWQI allows for preventing soil and water deterioration which is an essential issue in agricultural production. The IWQI values in groundwater samples are shown in Figure 8. As observed, the agricultural quality of water is low in western parts, suitable

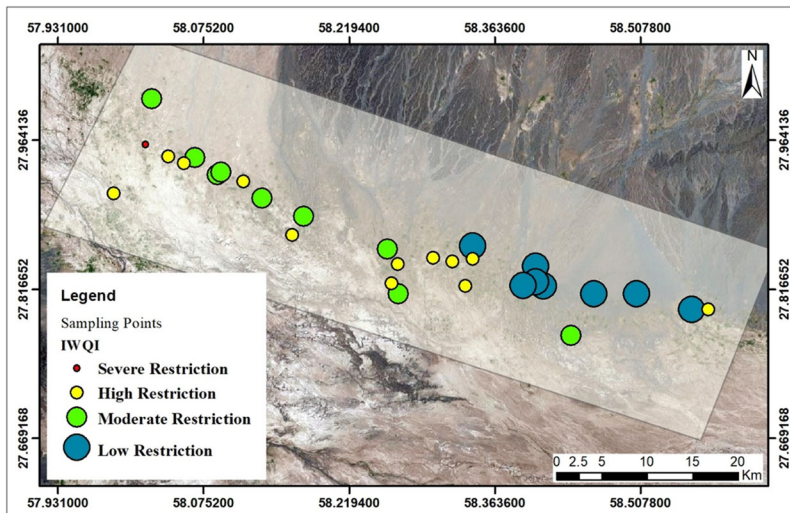


Figure 8. Spatial variation map of IWQI.

in the central parts, and moderate in the other parts. The average value of IWQI for samples is 58.3 which means moderate restriction of use for agriculture. The IWQI values demonstrate that eight samples (26.6%) lie at “low restriction” (70–85) class, nine samples (30%) at “moderate restriction” class (55–70), 12 samples (40%) at “high restriction” (40–55) class and 1 sample (3.3%) at “severe restriction” (40>) class. Accordingly, the highest numbers (40%) lie in the “high restriction” class. Therefore, the quality of groundwaters for agricultural purposes is low in general. Consequently, it is proposed that high permeability soils, lacking compact layers should be used for irrigation.

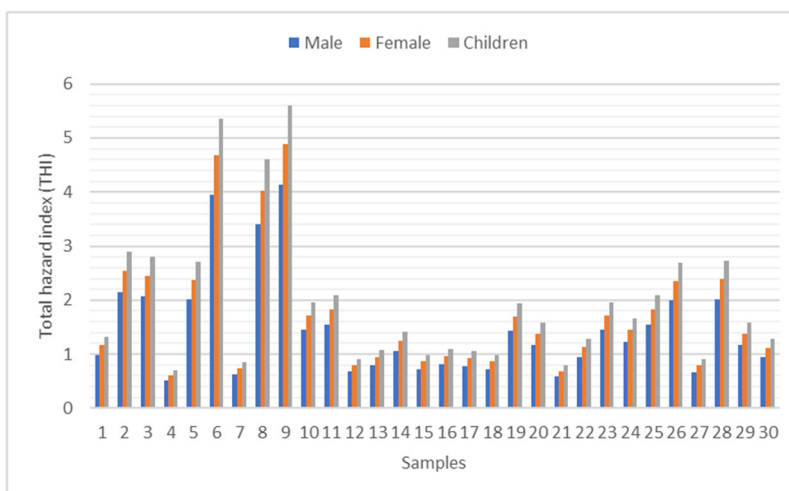
Health risk assessment

Many countries are concerned about the noncarcinogenic risks of F^- and NO_3^- in their groundwater resources (Nawale et al. 2021; Rezaei et al. 2017; Xiao et al. 2022). A lack of proper treatment could cause severe human health problems if waters with high concentrations of NO_3^- and F^- are consumed. In this study, the health impacts of F^- and NO_3^- were evaluated using hazard quotients. Based on the potential noncarcinogenic health risks of oral exposure to groundwater, the potential risks for adult males, adult females, and children are presented in Table 6. The values of $HQ_{nitrate}$ for males, females, and children were 0.844, 0.998, and 1.141, respectively. Meanwhile, the values of $HQ_{fluoride}$ for males, females, and children were 0.609, 0.720, and 0.823, respectively. According to USEPA guidelines (USEPA 2014), the acceptable risk for humans is below one ($HI < 1$). Therefore, 33.33, 40, and 50% of the samples impose the noncarcinogenic risk of nitrate consumption on males, females, and children, respectively.

Comparing data based on the mean values of HQ for nitrate and fluoride revealed the following noncarcinogenic risks: Children > females > males. Furthermore, nitrate poses a greater risk in the study area than fluoride.

Table 6. Hazard quotients and total hazard index for nitrate and fluoride in groundwater samples for male, female, and children (Hazard values greater than 1 are bolded).

Sample no.	HQ _{NO₃}			HQ _F			THI		
	Male	Female	Children	Male	Female	Children	Male	Female	Children
1	0.214	0.253	0.289	0.769	0.909	1.040	0.983	1.162	1.329
2	1.700	2.009	2.298	0.449	0.531	0.607	2.148	2.540	2.904
3	0.788	0.932	1.066	1.282	1.516	1.733	2.071	2.448	2.799
4	0.192	0.227	0.260	0.321	0.379	0.433	0.513	0.606	0.693
5	1.560	1.845	2.109	0.449	0.531	0.607	2.009	2.375	2.716
6	0.880	1.040	1.190	3.077	3.638	4.160	3.957	4.678	5.350
7	0.373	0.441	0.504	0.256	0.303	0.347	0.629	0.744	0.850
8	3.149	3.723	4.258	0.256	0.303	0.347	3.405	4.026	4.604
9	1.063	1.256	1.437	3.077	3.638	4.160	4.139	4.894	5.597
10	1.197	1.415	1.619	0.256	0.303	0.347	1.454	1.719	1.965
11	1.296	1.532	1.752	0.256	0.303	0.347	1.552	1.835	2.098
12	0.418	0.495	0.566	0.256	0.303	0.347	0.675	0.798	0.912
13	0.538	0.637	0.728	0.256	0.303	0.347	0.795	0.940	1.075
14	0.793	0.938	1.073	0.256	0.303	0.347	1.050	1.241	1.419
15	0.474	0.560	0.640	0.256	0.303	0.347	0.730	0.863	0.987
16	0.553	0.654	0.748	0.256	0.303	0.347	0.809	0.957	1.094
17	0.526	0.622	0.712	0.256	0.303	0.347	0.783	0.926	1.058
18	0.474	0.560	0.640	0.256	0.303	0.347	0.730	0.863	0.987
19	1.055	1.248	1.427	0.385	0.455	0.520	1.440	1.702	1.947
20	0.788	0.932	1.066	0.385	0.455	0.520	1.173	1.387	1.586
21	0.262	0.310	0.354	0.321	0.379	0.433	0.583	0.689	0.788
22	0.313	0.369	0.423	0.641	0.758	0.867	0.954	1.127	1.289
23	0.933	1.103	1.261	0.513	0.606	0.693	1.446	1.709	1.954
24	0.716	0.847	0.969	0.513	0.606	0.693	1.229	1.453	1.662
25	1.031	1.219	1.394	0.513	0.606	0.693	1.544	1.826	2.088
26	1.349	1.594	1.823	0.641	0.758	0.867	1.990	2.352	2.690
27	0.159	0.188	0.215	0.513	0.606	0.693	0.671	0.794	0.908
28	1.567	1.853	2.119	0.449	0.531	0.607	2.016	2.384	2.726
29	0.659	0.779	0.891	0.513	0.606	0.693	1.171	1.385	1.584
30	0.308	0.364	0.416	0.641	0.758	0.867	0.949	1.122	1.283
Min	0.16	0.19	0.21	0.26	0.30	0.35	0.51	0.61	0.69
Max	3.15	3.72	4.26	3.08	3.64	4.16	4.14	4.89	5.60
Mean	0.84	1.00	1.14	0.61	0.72	0.82	1.45	1.72	1.96

**Figure 9.** Total hazard index of fluoride and nitrate for children, female, and male in groundwater samples.

In this study, the excessive adverse health risks of fluoride and nitrate in drinking water were assessed through the THI, which was calculated as the sum of HQs for fluoride and nitrate. Table 6 and Figure 9 illustrate the THI for all groundwater samples to assess the risks for children, females, and males, respectively. The calculated THIs range from 0.513 to 4.139, 0.606 to 4.894, and 0.693 to 5.597 for men, women, and children, respectively. Accordingly, the average THI was 1.45, 1.72, and 1.96. In 30 groundwater samples, for children, women, and men, THI levels exceeded 1 ($\text{THI} > 1$) in 23 (76.67%), 20 (66.67%), and 17 (56.67%) samples, respectively.

According to THI results, children are more jeopardized by noncarcinogenic risks due to their physical condition and ingestion rate. Similar results were reported by Adimalla and Qian (2019); Qasemi et al. (2019); Haji et al. (2021).

Conclusion

In the present study, the quality of groundwater resources in the northern Jazmourian was assessed, and the following conclusions are drawn:

- According to the Piper diagram, Na is the most abundant cation, whereas, Cl and SO_4 are the most dominant anions and the major groundwater type is Na-Cl- SO_4 .
- The fluoride concentration ranges from 0.4 to 4.8 mg/L, with an average of 0.95 mg/L, and in three samples, F^- contents are higher than the threshold value suggested by WHO. Fluorite unsaturation and pH rise are considered the main factors influencing high- F values in some samples. Both these agents are the results of ion exchange in deltaic sediments.
- The nitrate concentration varied from 6.6 to 131 with a mean of 35.07 mg/L. NO_3^- content in 20% and 80% of samples exceed the WHO guideline for adults and children, respectively. Agricultural fertilizers are considered the main source of nitrate in groundwaters.
- Calculated WQI demonstrates that 43.33% of samples are “good” for human consumption, about 43.33% of samples are “poor” and 13.1% of samples are “very poor” in quality.
- IWQI values illustrate that groundwater quality for irrigation is good in the eastern part, poor in the west, and moderate in other parts of the studied area. Out of 30 analyzed samples, eight samples fall into the “low restriction” category, 9 and 12 samples are in the “moderate restriction” and “high restriction” categories, respectively, whereas only one sample is in the “severe restriction” category which is used for irrigation.
- Based on human health risk assessment, it is concluded that nitrate poses a greater risk than fluoride. The noncarcinogenic risks for both F^- and NO_3^- were calculated as children > female > male, respectively. The study revealed that THI ($\text{F}^- + \text{NO}_3^-$) of children, female and male have exceeded the acceptable limit in 76.67%, 66.67%, and 56.67% of samples, respectively.

The results of our study indicate that there is a need for additional research to determine the relative roles of natural and human factors and find ways to reduce the human health risk. Also, continuous monitoring and management for Jazmourian water catchment must be prioritized.

Acknowledgments


The authors wish to express their gratitude to the editor-in-chief and anonymous reviewers of *Human and Ecological Risk Assessment* journal.

Disclosure statement

The authors declare that they have no conflict of interest.

ORCID

Behnam Abbasnejad  <http://orcid.org/0000-0002-5993-0865>

Ahmad Abbasnejad  <http://orcid.org/0000-0001-7057-9108>

Reza Derakhshani  <http://orcid.org/0000-0001-7499-4384>

References

- Abbasnejad A, Mirzaie A, Derakhshani R, Esmaeilzadeh E. 2013. Arsenic in groundwaters of the alluvial aquifer of Bardsir plain, SE Iran. *Environ Earth Sci.* 69(8):2549–2557. doi:10.1007/s12665-012-2079-z
- Abbasnia A, Yousefi N, Mahvi AH, Nabizadeh R, Radfard M, Yousefi M, Alimohammadi M. 2019. Evaluation of groundwater quality using water quality index and its suitability for assessing water for drinking and irrigation purposes: case study of Sistan and Baluchistan province (Iran). *Hum Ecol Risk Assess.* 25(4):988–1005. doi:10.1080/10807039.2018.1458596
- Adimalla N, Li P. 2019. Occurrence, health risks, and geochemical mechanisms of fluoride and nitrate in groundwater of the rock-dominant semi-arid region, Telangana State, India. *Hum Ecol Risk Assess.* 25(1–2):81–103. doi:10.1080/10807039.2018.1480353
- Adimalla N, Li P, Qian H. 2019. Evaluation of groundwater contamination for fluoride and nitrate in semi-arid region of Nirmal Province, South India: a special emphasis on human health risk assessment (HHRA). *Hum Ecol Risk Assess.* 25(5):1107–1124. doi:10.1080/10807039.2018.1460579
- Adimalla N, Qian H. 2019. Hydrogeochemistry and fluoride contamination in the hard rock terrain of central Telangana, India: analyses of its spatial distribution and health risk. *SN Appl Sci.* 1(3):1–12. doi:10.1007/s42452-019-0219-8
- Adimalla N, Venkatayogi S. 2018. Geochemical characterization and evaluation of groundwater suitability for domestic and agricultural utility in semi-arid region of Basara, Telangana State, South India. *Appl Water Sci.* 8(1):1–14. doi:10.1007/s13201-018-0682-1
- Appelo CAJ, Postma D. 2004. *Geochemistry, groundwater and pollution*. AA Balkema, Rotterdam: CRC Press.
- Aravinthasamy P, Karunanidhi D, Subba Rao N, Subramani T, Srinivasamoorthy K. 2020. Irrigation risk assessment of groundwater in a non-perennial river basin of South India: implication from irrigation water quality index (IWQI) and geographical information system (GIS) approaches. *Arab J Geosci.* 13(21):1–14. doi:10.1007/s12517-020-06103-1
- Arshad N, Imran S. 2017. Assessment of arsenic, fluoride, bacteria, and other contaminants in drinking water sources for rural communities of Kasur and other districts in Punjab, Pakistan. *Environ Sci Pollut Res Int.* 24(3):2449–2463. doi:10.1007/s11356-016-7948-7

- Ayers RS, Westcot DW. 1985. Water quality for agriculture. Vol. 29. Rome: Food and Agriculture Organization of the United Nations Rome.
- Azhdarpoor A, Radfard M, Pakdel M, Abbasnia A, Badeenezhad A, Mohammadi AA, Yousefi M. 2019. Assessing fluoride and nitrate contaminants in drinking water resources and their health risk assessment in a semiarid region of southwest Iran. *DWT*. 149:43–51. doi:10.5004/dwt.2019.23865
- Bahrami M, Zarei AR, Rostami F. 2020. Temporal and spatial assessment of groundwater contamination with nitrate by nitrate pollution index (NPI) and GIS (case study: Fasarud Plain, southern Iran). *Environ Geochem Health*. 42(10):3119–3130. doi:10.1007/s10653-020-00546-x
- Bao Z, Hu Q, Qi W, Tang Y, Wang W, Wan P, Chao J, Yang XJ. 2017. Nitrate reduction in water by aluminum alloys particles. *J Environ Manage*. 196:666–673. doi:10.1016/j.jenvman.2017.03.080
- Bazeli J, Ghalehaskar S, Morovati M, Soleimani H, Masoumi S, Rahmani Sani A, Saghi MH, Rastegar A. 2020. Health risk assessment techniques to evaluate non-carcinogenic human health risk due to fluoride, nitrite and nitrate using Monte Carlo simulation and sensitivity analysis in Groundwater of Khaf County, Iran. *Int J Environ Anal Chem*. 102(8):1793–1813.
- Brown RM, McClelland NI, Deininger RA, Tozer RG. 1970. A water quality index-do we dare. *Water Sewage Works*. 117(10):339–343.
- Chen J, Gao Y, Qian H, Ren W, Qu W. 2021. Hydrogeochemical evidence for fluoride behavior in groundwater and the associated risk to human health for a large irrigation plain in the Yellow River Basin. *Sci Total Environ*. 800:149428. doi:10.1016/j.scitotenv.2021.149428
- Chen J, Wu H, Qian H. 2016. Groundwater nitrate contamination and associated health risk for the rural communities in an agricultural area of Ningxia, northwest China. *Expo Health*. 8(3): 349–359. doi:10.1007/s12403-016-0208-8
- Chen J, Wu H, Qian H, Gao Y. 2017. Assessing nitrate and fluoride contaminants in drinking water and their health risk of rural residents living in a semiarid region of Northwest China. *Expo Health*. 9(3):183–195. doi:10.1007/s12403-016-0231-9
- Chetty AA, Prasad S. 2016. Flow injection analysis of nitrate and nitrite in commercial baby foods. *Food Chem*. 197(Pt A):503–508. doi:10.1016/j.foodchem.2015.10.079
- Dehbandi R, Moore F, Keshavarzi B, Abbasnejad A. 2017. Fluoride hydrogeochemistry and bio-availability in groundwater and soil of an endemic fluorosis belt, central Iran. *Environ Earth Sci*. 76(4):1–15. doi:10.1007/s12665-017-6489-9
- Enalou HB, Moore F, Keshavarzi B, Zarei M. 2018. Source apportionment and health risk assessment of fluoride in water resources, south of Fars province, Iran: stable isotopes ($\delta^{18}\text{O}$ and δD) and geochemical modeling approaches. *Appl Geochem*. 98:197–205. doi:10.1016/j.apgeochem.2018.09.019
- Gangolli SD, Van Den Brandt PA, Feron VJ, Janzowsky C, Koeman JH, Speijers GJ, Spiegelhalder B, Walker R, Wishnok JS. 1994. Nitrate, nitrite and N-nitroso compounds. *Eur J Pharmacol Environ Toxicol Pharm*. 292(1):1–38.
- Haji M, Karuppanan S, Qin D, Shube H, Kawo NS. 2021. Potential human health risks due to groundwater fluoride contamination: a case study using multi-techniques approaches (GWQI, FPI, GIS, HHRA) in Bilate River Basin of Southern Main Ethiopian Rift, Ethiopia. *Arch Environ Contam Toxicol*. 80(1):277–293. doi:10.1007/s00244-020-00802-2
- Hameed A, Nazir S, Rehman JU, Ahmad N, Hussain A, Alam I, Nazir A, Tahir MB. 2021. Assessment of health hazards related to contaminations of fluorides, nitrates, and nitrites in drinking water of Vehari, Punjab, Pakistan. *Hum Ecol Risk Assess*. 27(6):1509–1522. doi:10.1080/10807039.2020.1858021
- Horton RK. 1965. An index number system for rating water quality. *J Water Pollut Control Fed*. 37(3):300–306.
- Jabbo JN, Isa NM, Aris AZ, Ramli MF, Abubakar MB. 2022. Geochemometric approach to groundwater quality and health risk assessment of heavy metals of Yankari Game Reserve and its environs, Northeast Nigeria. *J Cleaner Prod*. 330:129916. doi:10.1016/j.jclepro.2021.129916

- Khalaf RM, Hassan WH. 2013. Evaluation of irrigation water quality index IWQI for Al-Dammam confined aquifer in the west and southwest of Karbala city, Iraq. *Int J Civil Eng IJCE*. 23:21–34.
- Khalid S. 2019. An assessment of groundwater quality for irrigation and drinking purposes around brick kilns in three districts of Balochistan province, Pakistan, through water quality index and multivariate statistical approaches. *J Geochem Explor*. 197:14–26. doi:10.1016/j.gexplo.2018.11.007
- Kumar P. 2021. Groundwater fluoride contamination in Coimbatore district: a geochemical characterization, multivariate analysis, and human health risk perspective. *Environ Earth Sci*. 80(6): 1–14. doi:10.1007/s12665-021-09521-w
- Li P, Li X, Meng X, Li M, Zhang Y. 2016. Appraising groundwater quality and health risks from contamination in a semiarid region of northwest China. *Expo Health*. 8(3):361–379. doi:10.1007/s12403-016-0205-y
- Meireles ACM, Andrade Emd, Chaves LCG, Frischkorn H, Crisostomo LA. 2010. A new proposal of the classification of irrigation water. *Rev Ciênc Agron*. 41(3):349–357. doi:10.1590/S1806-66902010000300005
- Mukherjee I, Singh UK. 2018. Groundwater fluoride contamination, probable release, and containment mechanisms: a review on Indian context. *Environ Geochem Health*. 40(6):2259–2301. doi:10.1007/s10653-018-0096-x
- Murray J. 1986. Appropriate use of fluorides for human health. Geneva: World Health Organization.
- Nawale V, Malpe D, Marghade D, Yenkie R. 2021. Non-carcinogenic health risk assessment with source identification of nitrate and fluoride polluted groundwater of Wardha sub-basin, central India. *Ecotoxicol Environ Saf*. 208:111548. doi:10.1016/j.ecoenv.2020.111548
- Nazerizadeh N. 2017. Study report on extending the restriction of Rudbar area. South Rudbar water resources report (in Persian). Regional Water Organization of Kerman Province, Iran, 131 p.
- Qasemi M, Afsharnia M, Farhang M, Ghaderpoori M, Karimi A, Abbasi H, Zarei A. 2019. Spatial distribution of fluoride and nitrate in groundwater and its associated human health risk assessment in residents living in Western Khorasan Razavi, Iran. *DWT*. 170:176–186. doi:10.5004/dwt.2019.24691
- Qasemi M, Farhang M, Morovati M, Mahmoudi M, Ebrahimi S, Abedi A, Bagheri J, Zarei A, Bazeli J, Afsharnia M, et al. 2022. Investigation of potential human health risks from fluoride and nitrate via water consumption in Sabzevar, Iran. *Int J Environ Anal Chem*. 102(2): 307–318. doi:10.1080/03067319.2020.1720668
- Rajasooriyar LD, Boelee E, Prado MC, Hiscock KM. 2013. Mapping the potential human health implications of groundwater pollution in southern Sri Lanka. *Water Resour Rural Dev*. 1–2: 27–42. doi:10.1016/j.wrr.2013.10.002
- Rezaei H, Jafari A, Kamarehie B, Fakhri Y, Ghaderpoury A, Karami MA, Ghaderpoori M, Shams M, Bidarpoor F, Salimi M. 2019. Health-risk assessment related to the fluoride, nitrate, and nitrite in the drinking water in the Sanandaj, Kurdistan County, Iran. *Hum Ecol Risk Assess*. 25(5):1242–1250. doi:10.1080/10807039.2018.1463510
- Rezaei M, Nikbakht M, Shakeri A. 2017. Geochemistry and sources of fluoride and nitrate contamination of groundwater in Lar area, south Iran. *Environ Sci Pollut Res Int*. 24(18): 15471–15487. doi:10.1007/s11356-017-9108-0
- Singh A, Patel AK, Kumar M. 2020. Mitigating the risk of arsenic and fluoride contamination of groundwater through a multi-model framework of statistical assessment and natural remediation techniques. In: *Emerging issues in the water environment during Anthropocene*. Singapore: Springer. p. 285–300.
- Su H, Kang W, Li Y, Li Z. 2021. Fluoride and nitrate contamination of groundwater in the Loess Plateau, China: sources and related human health risks. *Environ Pollut*. 286:117287. doi:10.1016/j.envpol.2021.117287

- Toolabi A, Bonyadi Z, Paydar M, Najafpoor AA, Ramavandi B. 2021. Spatial distribution, occurrence, and health risk assessment of nitrate, fluoride, and arsenic in Bam groundwater resource, Iran. *Groundwater Sustain Dev.* 12:100543. doi:[10.1016/j.gsd.2020.100543](https://doi.org/10.1016/j.gsd.2020.100543)
- USEPA. 2014. Human Health Evaluation Manual, Supplemental Guidance: update of Standard Default Exposure Factors-OSWER Directive 9200. USA, 1–120.
- WHO. 2017. Guidelines for drinking-water quality: first addendum to the fourth edition. *J. Am. Water Works Assoc.* (109):44–51.
- Xiao Y, Hao Q, Zhang Y, Zhu Y, Yin S, Qin L, Li X. 2022. Investigating sources, driving forces and potential health risks of nitrate and fluoride in groundwater of a typical alluvial fan plain. *Sci Total Environ.* 802:149909. doi:[10.1016/j.scitotenv.2021.149909](https://doi.org/10.1016/j.scitotenv.2021.149909)
- Zhang B, Zhao D, Zhou P, Qu S, Liao F, Wang G. 2020. Hydrochemical characteristics of groundwater and dominant water–rock interactions in the Delingha Area, Qaidam Basin, Northwest China. *Water.* 12(3):836. doi:[10.3390/w12030836](https://doi.org/10.3390/w12030836)